Biochemical Pharmacology 81 (2011) 594–605

Contents lists available at ScienceDirect

Biochemical Pharmacology

journal homepage: www.elsevier.com/locate/biochempharm

Autophagy inhibition enhances apoptosis triggered by BO-1051, an N-mustard derivative, and involves the ATM signaling pathway

Li-Hsin Chen [a], Che-Chuan Loong [b], Tsann-Long Su [c], Yi-Jang Lee [d], Pei-Ming Chu [e], Ming-Long Tsai [f], Ping-Hsin Tsai [a], Pang-Hsien Tu [c], Chin-Wen Chi [a,g], Hsin-Chen Lee [a,1], Shih-Hwa Chiou [a,g,1,*]

[a] Department and Institute of Pharmacology, School of Medicine, National Yang-Ming University, 155, Sec 2, Linong Street, Taipei 112, Taiwan
[b] Department of Surgery, Division of Transplantation Surgery, Taipei Veterans General Hospital, 201, Sec 2, Shih-Pai Road, Taipei 112, Taiwan
[c] Institute of Biomedical Sciences, Academia Sinica, 128, Academia Road, Sec 2, Taipei 115, Taiwan
[d] Department of Biomedical Image and Radiological Sciences, School of Biomedical Science and Engineering, National Yang-Ming University, 155, Sec 2, Linong Street, Taipei 112, Taiwan
[e] Graduate Institutes of Life Sciences, National Defense Medical Center, 161, Sec 6, Minquan E. Road, Taipei 114, Taiwan
[f] Institute of Clinical Medicine, School of Medicine, National Yang-Ming University, 155, Sec 2, Linong Street, Taipei 112, Taiwan
[g] Department of Medical Research and Education, Taipei Veterans General Hospital, 201, Sec 2, Shih-Pai Road, Taipei 112, Taiwan

ARTICLE INFO

Article history:
Received 30 September 2010
Accepted 10 December 2010
Available online 22 December 2010

Keywords:
N-mustard
Apoptosis
Autophagy
ATM
Hepatoma

ABSTRACT

In a previous study, BO-1051, an N-mustard linked with a DNA-affinic molecule, was shown to target various types of cancer cell lines. In the present study, we aimed to investigate the cytotoxicity, as well as the underlying mechanism, of BO-1051. We found that BO-1051 simultaneously induced apoptosis and autophagy in hepatocellular carcinoma cell lines. DNA double strand breaks induced by BO-1051 activated the ATM signaling pathway and subsequently resulted in caspase-dependent apoptosis. When autophagy was inhibited in its early or late stages, apoptosis was significantly enhanced. This result indicated autophagy as a cytoprotective effect against BO-1051-induced cell death. We further inhibited ATM activation using an ATM kinase inhibitor or ATM-specific siRNA and found that while apoptosis was blocked, autophagy also diminished in response to BO-1051. We not only determined a signaling pathway induced by BO-1051 but also clarified the linkage between DNA damage-induced apoptosis and autophagy. We also showed that BO-1051-induced autophagy acts as a cytoprotective reaction and downstream target of the ATM-signaling pathway. This research revealed autophagy as a universal cytoprotective response against DNA damage-inducing chemotherapeutic agents, including BO-1051, cisplatin, and doxorubicin, in hepatocellular carcinoma cell lines. Autophagy contributes to the remarkable drug resistance ability of liver cancer.

1. Introduction

DNA bifunctional alkylating agents containing a mustard moiety belong to an important class of antitumor drugs. The mustard derivatives are capable of crosslinking DNA double strands but lack the affinity to bind DNA, which precludes them from being effective antitumor agents. This drawback has been improved by adding a DNA-affinic carrier to the original mustard derivatives. The newly synthesized molecules showed higher cytotoxicity and therapeutic efficacy as compared to the corresponding untargeted mustards of similar reactivity [1–3].

Klionsky et al. designed and synthesized a series of N-mustard derivatives of 9-anilinoacridine based on the evidence mentioned. In the previous study, BO-1051 (Fig. S1) showed remarkable ability to target a variety of cancer cell lines, including two drug-resistant cell lines [4]. In in vivo experiments, BO-1051 was demonstrated to have potent antitumor efficacy in nude mice bearing human breast MX-1 xenografts. BO-1051 could also effectively suppress human glioma U87MG xenografts in nude mice [4]. The underlying mechanism of cell death induced by BO-1051, however, was not determined.

Macroautophagy (henceforth referred to as autophagy) is considered as programmed cell death type II, which occurs in certain situations and results in cell death [5–7]. Nevertheless, more evidence has revealed that autophagy is a novel response of cancer cells against various types of stress [8–10]. Inhibition at different stages in the process of autophagy may also lead to different consequences [11]. Despite studies showing that genotoxic stress can activate autophagy [8,12], direct links between DNA damage and autophagy are still lacking.

* Corresponding author at: Department and Institute of Pharmacology, School of Medicine, National Yang-Ming University, 155, Sec 2, Linong Street, Taipei 112, Taiwan. Tel.: +886 2 2875 7394; fax: +886 2 2871 0773.
E-mail address: shchiou@vghtpe.gov.tw (S.-H. Chiou).
[1] These authors contributed equally to this study.

0006-2952/$ – see front matter © 2011 Elsevier Inc. All rights reserved.
doi:10.1016/j.bcp.2010.12.011

The aim of the present study was to determine the molecular mechanism of BO-1051 and the crosstalk between autophagy and apoptosis in BO-1051-induced cytotoxicity. We focused our attention on hepatocellular carcinoma (HCC)-derived cell lines due to the poor prognosis and lack of effective therapies in treating hepatocarcinoma, except liver transplantation. Our results indicate that BO-1051 induced autophagy in early stages and acted as a defense system against apoptosis. Inhibition of autophagy in its early or late stages resulted in an increase in the number of annexin V-positive cells. BO-1051-induced autophagy has a cytoprotective role and is connected to the ATM signaling pathway. This research revealed autophagy as a universal cytoprotective response against DNA damage-inducing chemotherapeutic agents, including BO-1051, cisplatin, and doxorubicin, in hepatocellular carcinoma cell lines. Therefore, autophagy contributes to the remarkable drug resistance ability of liver cancer.

2. Materials and methods

2.1. Materials

BO-1051 was a gift synthesized by Su [4]; the compound was numbered 24d in the previous literature. The chemical structure of BO-1051 is shown in Fig. S1. Acridine orange, E64d, pepstatin A, bafilomycin A1, chloroquine, methylpyruvate, doxorubicin, and cisplatin were purchased from Sigma Chemical Co. (St. Louis, MO, USA). Z-VAD-fmk was purchased from Promega (Madison, WI, USA). ATM kinase inhibitor, Chk1 inhibitor, and Chk2 inhibitor II were purchased from Merck (Darmstadt, Germany).

2.2. Cell lines and culture

HA22T/VGH and Mahlavu cells are both poorly differentiated human hepatoma cell lines. They were obtained from the Bioresource Collection and Research Center (BCRC) in the Food Industry Research and Development Institute (Hsinchu, Taiwan) and were cultured in Dulbecco's modified eagle medium (GIBCO, Grand Island, NY, USA), with 10% fetal bovine serum (GIBCO), 100 U/ml penicillin, and 100 μg/ml streptomycin (GIBCO) under standard culture conditions (37 °C, 95% humidified air and 5% CO_2).

2.3. MTT assay

Cells were seeded in 96-well (6000 cells per well) or 24-well plates (30,000 cells per well) in complete culture medium. After overnight culture, the medium was replaced with either solvent or chemicals at indicated concentrations in complete medium. The cells were cultured until the time indicated, and the MTT assay was then performed. In brief, cells were stained with 0.1 mg/ml MTT (Sigma) for 2–4 h and then dissolved in DMSO (Sigma). MTT values were measured at 570 nm using a microplate reader.

2.4. Detection of acidic vesicular organelles (AVO) with acridine orange

To quantify the development of AVOs in BO-1051-treated cells, cells were stained with acridine orange (Sigma), and the intensity of the red fluorescence was measured by flow cytometry. Green (510–530 nm) and red (>650 nm) fluorescence emission from 10,000 cells illuminated with blue (488 nm) excitation light was measured with a FACSCalibur from Becton Dickinson (San Jose, CA, USA) using CellQuest Software.

2.5. Immunofluorescence staining

Briefly, cells were sub-cultured in a 4-well Lab-Tek chambered coverglass system (Nalge Nunc, Rochester, NY) for 24 h. After overnight cultured, cells were treated with BO-1051 in complete culture medium for indicated times. Then, cells were fixed with 4% paraformaldehyde (Sigma), permeabilized with 0.1% Triton X-100 (Sigma), immunostained with indicated antibodies, and labelled with FITC-conjugated secondary antibodies that allowed for fluorescent imaging. The LC-3 antibody was purchased from Novus Biologicals (Littleton, CO, USA) and the γH2AX antibody was purchased from Millipore Corporation (Bedford, MA, USA).

2.6. Immunoblotting

Harvested cells were pelleted by centrifugation, washed with PBS, and lysed with RIPA buffer. Protein content was measured with a protein assay kit (Bio-Rad Laboratories, Hercules, CA, USA). Fifty micrograms of total protein were separated by SDS/PAGE (10% or 12% gels) and transferred to nitrocellulose membranes (Pall Corporation, MI, USA) for immunological detection of proteins. The blots were probed using antibodies against LC3 (Novus Biologicals or Cell Signaling), ATG5 (Novus), Beclin 1 (Sigma), p62 (Progen biotechnik, Heidelberg, Germany), p-Chk1, p-Chk2, cleaved PARP, cleaved caspase-3, cleaved caspase-7 (Cell Signaling Technology, Beverly, MA, USA), tubulin (Abcam, Cambridge, MA, USA), p-Rad17 (Montgomery, TX, USA), p-ATM, γH2AX, and beta-actin (Millipore Corporation, Milford, MA, USA).

2.7. Apoptosis assays

Both FITC-conjugated annexin V and terminal deoxynucleotidyl transferase dUTP nick end labelling (TUNEL) assays (Roche, Palo Alto, CA) were used to determine the presence of apoptosis. Cells were seeded in a 6-cm dish one day before BO-1051 treatment. After BO-1051 treatment for the indicated time, cells were harvested and stained with annexin V-FITC and PI (BD Falcon, Bedford, MA, USA) or labelled using the TUNEL assay (Roche) according to the manufacturer's instructions. Both annexin V and TUNEL staining were detected by flow cytometry.

2.8. shLuc and shBECN1 expression construct and lentiviral transduction

The stable ablation of Beclin1 in HCC cell lines was obtained using small hairpin RNA (shRNA) probes for the *Homo sapiens* gene beclin 1 (BECN1): TRCN0000033549 (shBECN1 A01) and TRCN0000033550 (shBECN1 B01). Control cells stably expressed shLuc (pLKO.1-shLuc). Cells were infected with shRNA lentiviruses generated using a three-plasmid-based lentivirus system (all plasmids are available from the RNAi Consortium [TRC]). Lentivirus production was performed by transfection of 293T cells at 5×10^6 cells per 10 cm plate using Lipofectamine 2000 (LF2000, Invitrogen Life Technologies, Carlsbad, CA, USA). Supernatants were collected 48 h after transfection and then were filtered. Subconfluent cells were infected with lentivirus in the presence of 8 μg/ml polybrene (Sigma). Infected cells were selected with puromycin (2 μg/ml) until control uninfected cells were completely dead. Immunoblotting was used to confirm the knockdown efficiency of shBECN1.

2.9. siRNA transfection

On-TARGETplus siRNA smart pools for nontargeting control, p62/SQSTM1 (NM_003900), and ATM (NM_138292) were purchased from Dharmacon Research (Lafayette, CO, USA). Transient transfection was carried out using INTERFERin™ siRNA transfection reagent (Polyplus Transfection, Huntingdon, UK) according to the manufacturer's guide. Two days after transfection, cells were treated with BO-1051 for further experiments.

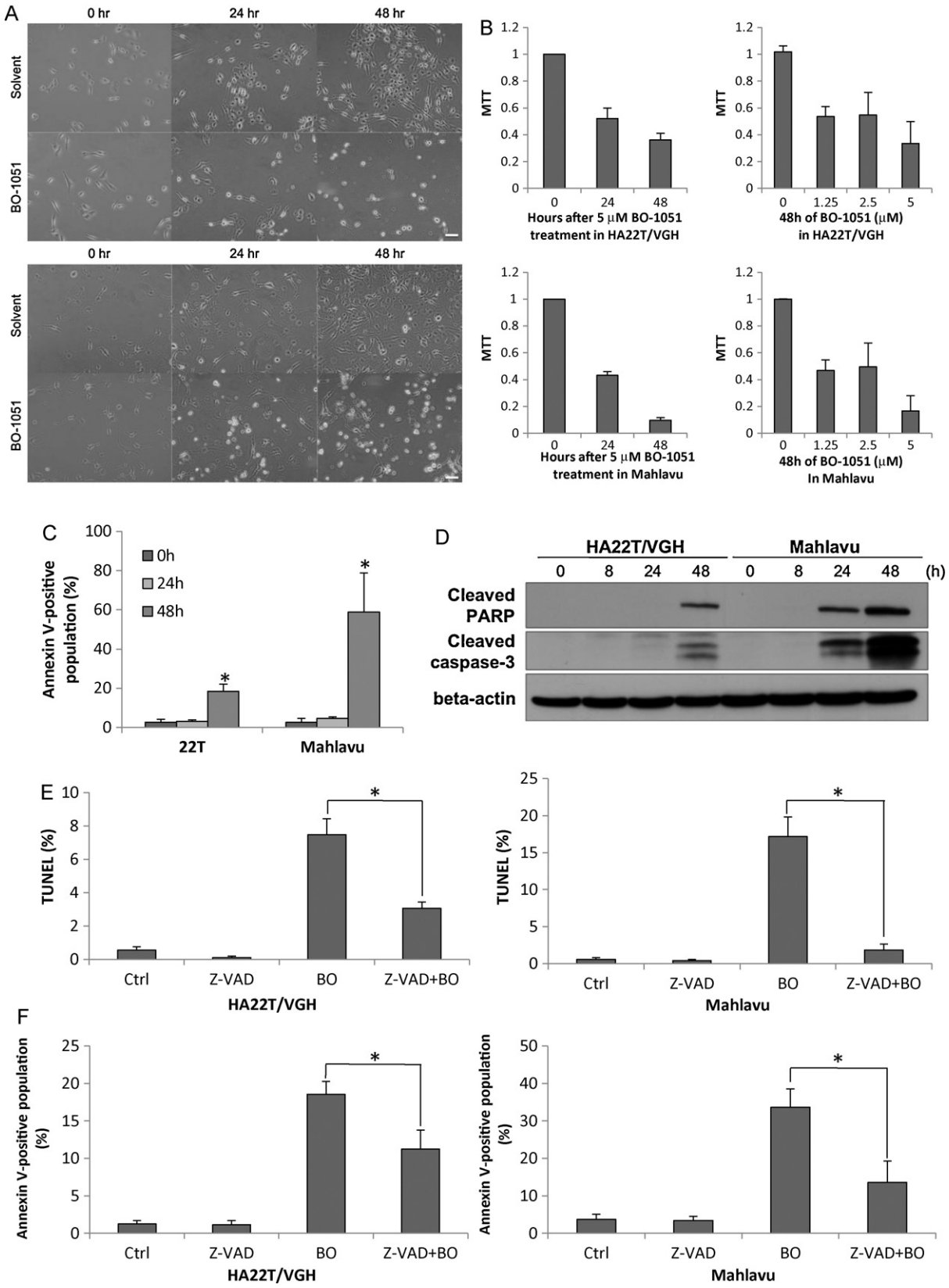

Fig. 1. Toxicity and apoptotic effect of BO-1051. (A) HA22T/VGH (upper panel) and Mahlavu (lower panel) cells were treated with either solvent or 5 μM BO-1051. After 0, 24, or 48 h, cell morphology was observed. (B) HA22T/VGH (upper panel) and Mahlavu (lower panel) cells were treated with indicated concentrations of BO-1051. After 0, 24, or 48 h, MTT assays were performed as detailed in Section 2 to determine the cytotoxicity of BO-1051. Data are expressed as the ratio (mean ± SD) of the control. (C) HA22T/VGH and Mahlavu cells were treated with 5 μM BO-1051 for 0, 24 or 48 h. Cells were then stained with annexin V-FITC and propidium iodide (PI) and subsequently analyzed by flow cytometry. Only annexin V-positive cells were counted as apoptotic cells. (D) HA22T/VGH and Mahlavu cells were treated with 5 μM BO-1051 for the indicated times. Proteins extracted from harvested cells were resolved by SDS-PAGE, transferred to nitrocellulose and probed with cleaved PARP- and cleaved caspase-3-specific antibodies. (E) HA22T/VGH (left) and Mahlavu (right) cells were treated with 5 μM BO-1051 in the presence or absence of Z-VAD-fmk (20 μM), a pan caspase inhibitor. Cells were then fixed, and the TUNEL assay was used to evaluate the percentage of cells with DNA fragmentation. (F) HA22T/VGH (left) and Mahlavu (right) cells were treated with 5 μM BO-1051 for 48 h. Cells were then

2.10. Data analysis

Data were expressed as mean ± SD from at least three independent experiments. Statistical analysis was performed using Student's *t*-test. A difference was considered significant when $p < 0.05$.

3. Results

3.1. Cytotoxic effects of BO-1051 on HCC cell lines and morphological features of BO-1051-treated cells

To determine the cytotoxic effects of BO-1051 in human HCC cell lines, HA22T/VGH and Mahlavu cells were treated with 5 μM BO-1051. After 0, 24, and 48 h, cell morphology was observed by photography. Significant cell death was observed 48 h after BO-1051 treatment (Fig. 1A). In addition, dose–response and time–response studies were performed by MTT assay. As shown in Fig. 1B, BO-1051 inhibited growth in both dose-dependent and time-dependent manners in HA22T/VGH and Mahlavu cells. Other HCC cell lines were also treated with BO-1051 to determine their IC_{50} values. As shown in Table S1, the IC_{50} values of BO-1051 in various liver cancer cell lines were below 5 μM.

After treatment with BO-1051 for 48 h, cells displayed characteristic apoptotic changes in their morphology, including plasma membrane blebbing, cell shrinkage, and the formation of apoptotic bodies. Moreover, in some cell lines, including Mahlavu and SK-Hep1 cells but not HA22T/VGH cells, various numbers of vacuoles were observed in the cytoplasm as few as 3 h after BO-1051 treatment (Fig. S2). The size and numbers of vacuoles within the cells increased with time and persisted until the cell died. The formation of vacuoles in BO-1051-treated cells are similar to those in cells undergoing autophagy [13], a general phenomenon that occurs when cells response to stress. We sought to examine the markers and time course of both apoptosis and autophagy in cells treated with BO-1051.

3.2. BO-1051-induced cell death is apoptosis

First, we examined if BO-1051-induced cell death is a typical apoptotic process. Annexin V staining showed an increased percentage of cells displaying phosphatidyl serine (PS) externalization (Fig. 1C) in both Mahlavu and HA22T/VGH cells. This significant change occurred 48 h after BO-1051 treatment. Cleaved PARP and cleaved caspase-3 were also detected in HA22T/VGH and Mahlavu cells treated with BO-1051 for 48 h (Fig. 1D). These data suggest that BO-1051 induces apoptosis in liver cancer cell lines.

Cells were then treated with BO-1051 in the presence or absence of Z-VAD-fmk, a pan caspase inhibitor, to confirm that the apoptosis pathway is involved in BO-1051-induced cell death. As shown in Fig. 1E, the percentage of TUNEL-positive cells treated with BO-1051 in the presence of Z-VAD-fmk was significantly decreased. The expression of cleaved-PARP and the percentage of annexin V-positive cells were also significantly decreased (Figs. S3 and 1F). Therefore, BO-1051 results in cell death through a caspase-dependent apoptosis pathway.

3.3. Apoptosis through the ATM-signaling pathway

Because BO-1051 was designed to target DNA [1] and results in DNA fragmentation as detected by a comet assay [4], we performed immunostaining to detect the expression of γH2AX, a marker for DNA double strand breaks (DSBs). Both HA22T/VGH and Mahlavu cells significantly expressed γH2AX 24 h after BO-1051 was added to the culture medium (Fig. 2A and B).

We then immunoblotted for several proteins that participated in the DNA DSB signaling pathway, including p-ATM, p-Chk2, p-Rad17, and γH2AX. The expression levels of these proteins were increased in correlation with the dosage of BO-1051 (Fig. 2C). To confirm if apoptosis was induced by DNA damage, we used an ATM specific inhibitor to block the activation of the DNA damage signaling pathway. The expression levels of cleaved PARP, cleaved caspase-3, and cleaved caspase-7 were significantly decreased in cells treated with BO-1051 and the ATM kinase inhibitor as compared to treatment with BO-1051 alone (Fig. 2D). As shown in Fig. 2E and F, combined treatment with the ATM kinase inhibitor and BO-1051 decreased the annexin V-positive population. Similarly, the annexin V-positive population decreased when a Chk2 inhibitor was applied (Fig. 2G and H). Therefore, from the data above, we conclude that BO-1051 induces apoptosis through ATM activation after DNA damage.

3.4. Induction of autophagy in BO-1051-treated HCC cell lines

We have proven that BO-1051 induces apoptosis in two HCC cancer cell lines. Nevertheless, autophagy is a type II programmed cell death in certain circumstances [5–7]. To determine whether BO-1051 also induces autophagy, the development of acidic vesicular organelles (AVOs), a characteristic of autophagy, was evaluated using acridine orange staining in Mahlavu and HA22T/VGH cells. As shown in Fig. 3A, there was an increase in red fluorescence in Mahlavu cells after BO-1051 treatment. We then used flow cytometry to quantify the staining. BO-1051 treatment increased red fluorescence (*y*-axis) in both Mahlavu and HA22T/VGH cells, indicating that the formation of AVOs was induced (Fig. 3B).

Next, we detected the formation of LC3 puncta, which are a specific feature of autophagy. As shown in Fig. 3C, Mahlavu and HA22T/VGH cells were treated with BO-1051 for 24 h and then immunostained with a LC3 antibody. A significant change in cytoplasmic LC3 puncta formation was observed in both cell lines, which indicated that autophagosomes formed in cells treated with BO-0151. Increased LC3-II maturation (the conversion of LC3-I into LC3-II) (Fig. 3D) was found as soon as 8 h after BO-1051 treatment. In addition, the p62/SQSTM1 protein serves as a link between LC3 and an ubiquitinated substrate. The reduction of p62/SQSTM1, another biochemical sign of autophagy, was also detected after treatment with BO-1051 and further suggests that autophagy was induced (Fig. 3D).

Nevertheless, the accumulation of autophagosomes and autophagolysosomes after BO-1051 treatment could involve an enhanced autophagic sequestration or a reduced degradation of autophagic material [14]. To distinguish between these two possibilities, we assessed BO-1051-induced autophagic vacuolization by adding two lysosomal protease inhibitors, E64d and pepstatin A. As shown in Fig. 3E, the inclusion of lysosomal protease inhibitors further increased the BO-1051-triggered induction of LC3-II. These data suggest that BO-1051 treatment increased autophagic activity, which also called as on-rate autophagic flux.

3.5. BO-1051-induced autophagy differs from typical autophagic cell death

In order to clarify the role of BO-1051-induced autophagy in liver cancer cell lines, bafilomycin A1 was used in the experiments. Bafilomycin A1 (BafA1) is an inhibitor of vacuolar ATPase (V-ATPase), and it prevents the fusion between lysosomes and

stained with annexin V-FITC and propidium iodide (PI) and subsequently analyzed by flow cytometry. Data represent the mean ± SD for at least three independent experiments. $^{*}p < 0.05$. Bar = 100 μm.

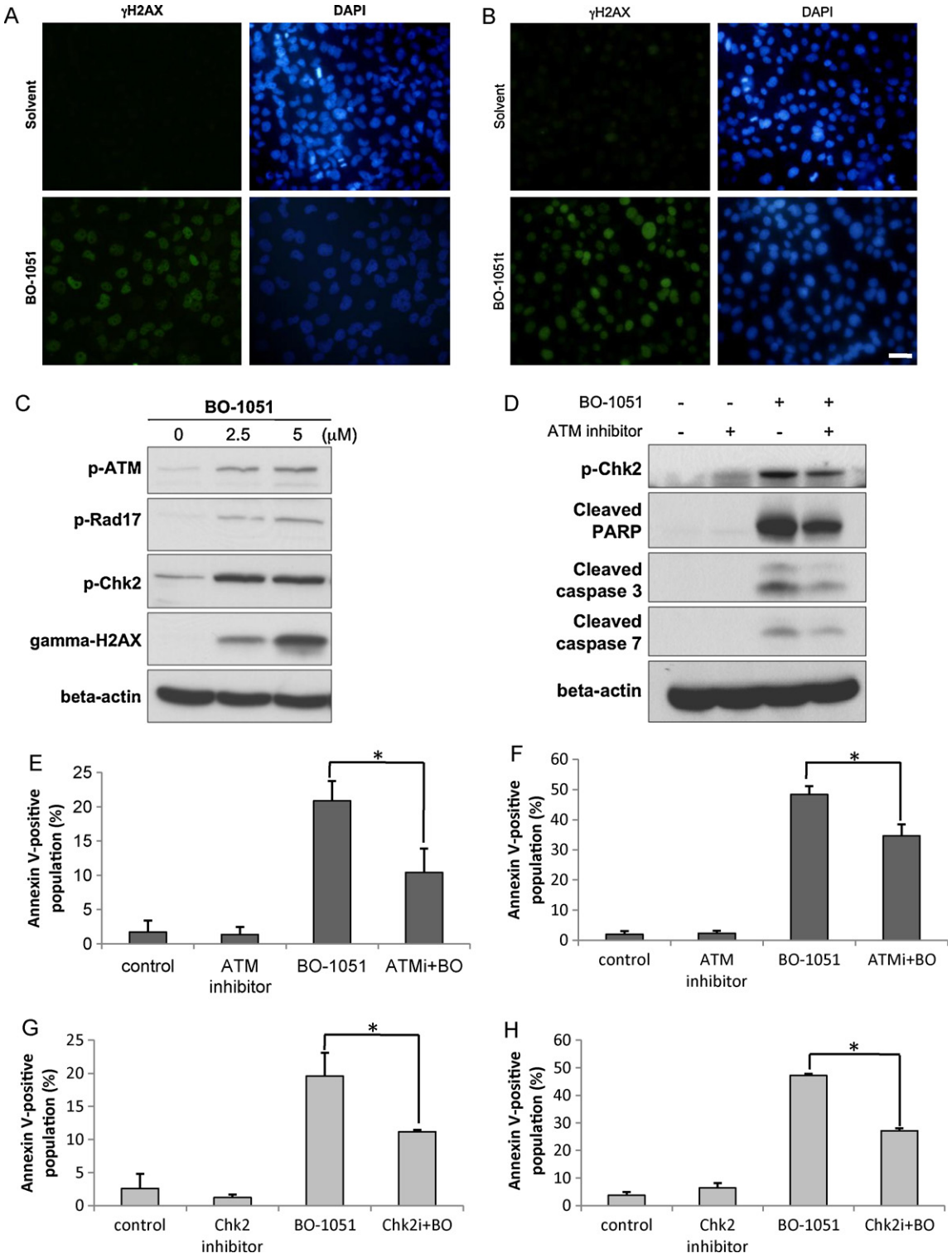

Fig. 2. BO-1051 induced apoptosis through the DNA damage pathway. (A) HA22T/VGH and (B) Mahlavu cells were treated with solvent or 5 μM BO-1051 for 24 h, followed by immunostaining of γH2AX (green fluorescence) and DAPI (blue fluorescence). (C) HA22T/VGH cells were treated with 0, 2.5, or 5 μM BO-1051 for 48 h, and isolated proteins were then subjected to immunoblotting with indicated antibodies. (D) HA22T/VGH cells were treated with solvent or 5 μM BO-1051 in the presence or absence of an ATM kinase inhibitor (10 μM), and then protein extracts were subjected to immunoblotting with indicated antibodies. (E) HA22T/VGH and (F) Mahlavu cells were treated with solvent or BO-1051 (5 μM) in the presence or absence of ATM kinase inhibitor for 48 h and then stained with annexin V-FITC and PI. (G) HA22T/VGH cells and (H) Mahlavu cells were treated with solvent or BO-1051 (5 μM) in the presence or absence of Chk2 inhibitor II (2 μM) for 48 h and then stained with annexin V and PI. Data represent the mean ± SD for at least three independent experiments. $^{*}p < 0.05$. Bar = 100 μm. (For interpretation of the references to color in this figure legend, the reader is referred to the web version of the article.)

autophagosomes. As shown in Fig. 4A, Mahlavu and HA22T/VGH cells were pretreated with BafA1 for 24 h, following with 0, 1.25, 2.5, or 5 μM BO-1051 for 48 h. Cells pretreated with BafA1 were more susceptible to low (1.25 and 2.5 μM) but not high (5 μM) doses of BO-1051.

We also applied shRNA to knockdown Beclin-1, which is an important protein that participates the formation of autophagosomes. We confirmed the knockdown efficiency of shRNA as shown in Fig. S4. The expression level of cleaved PARP and cleaved caspase-7 increased when Beclin-1 was knocked down in BO-

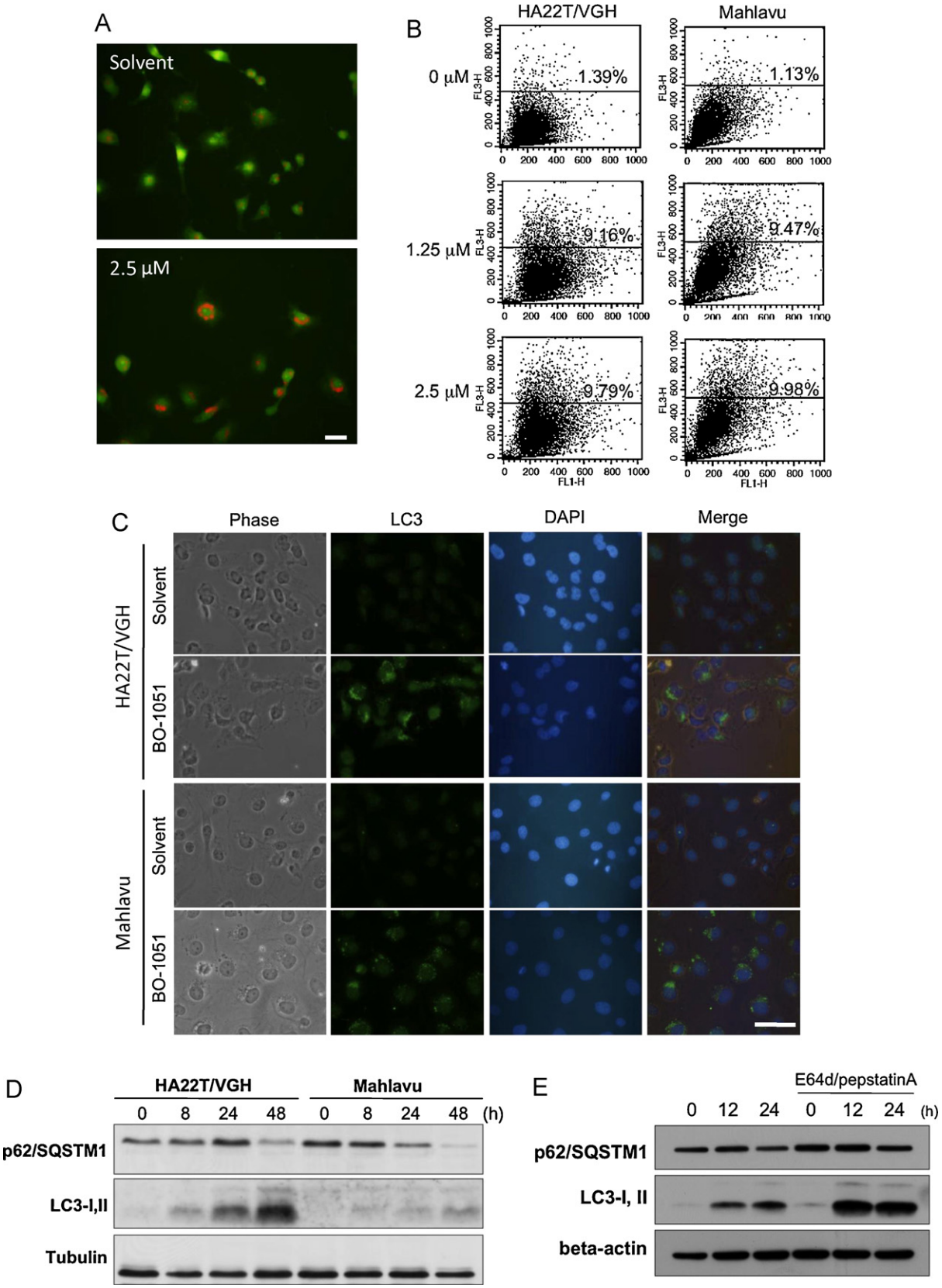

Fig. 3. Induction of autophagy in BO-1051-treated cells. (A) Mahlavu cells were treated with 0 or 2.5 μM BO-1051 and stained with acridine orange. Red fluorescence indicates the induction of AVOs. (B) HA22T/VGH (left) and Mahlavu (right) cells were exposed to 0, 1.25, or 2.5 μM BO-1051 for 48 h. FL1-H indicated green color intensity (cytoplasm and nucleus), while FL3-H shows red color intensity (AVO). (C) HA22T/VGH (upper panel) and Mahlavu (lower panel) cells were treated with solvent or 5 μM BO-1051 for 24 h, followed by immunostaining of LC-3 (green fluorescence) and DAPI (blue fluorescence). (D) Mahlavu and HA22T/VGH cells were treated with 5 μM BO-1051 for 0, 8, 24, or 48 h, and then extracted proteins were immunoblotted to detect LC3 and p62/SQSTM1 abundance. (E) HA22T/VGH cells were treated with BO-1051 5 μM for the indicated time, and then extracted proteins were immunoblotted with p62/SQSTM1 and LC3 antibodies. E64d (10 μg/ml) and pepstatin A (10 μg/ml) were added to the medium where indicated. Data are representative of three independent experiments. Bar = 100 μm. (For interpretation of the references to color in this figure legend, the reader is referred to the web version of the article.)

1051-treated cells (Fig. 4B). A similar result was obtained in the annexin V staining assay. Cells knocked down with shBECN1 showed an increased percentage of annexin V-positive cells (Fig. 4C). Therefore, inhibition of autophagy could not prevent cell death, but further enhanced the toxicity of BO-1051. Instead of autophagic cell death, these results indicate that autophagy had a cytoprotective effect in liver cancer cell lines in response to BO-1051 treatment.

Lum et al. have demonstrated that methylpyruvate (MP), a cell-permeable intermediate of glucose metabolism, can rescue cells from autophagy inhibition by providing fuel for the TCA cycle [15]. In our experiments, we applied MP to investigate whether cells provided with an energy source to maintain their energetic status would delay or inhibit the apoptosis induced by BO-1051. As shown in Fig. 4D, MP was added to the culture medium 24 h before analysis and was sufficient to reduce the annexin V-positive population in the shBECN1 group to the level of the shLuc control. Therefore, autophagy induced by BO-1051 reduced apoptosis by providing metabolic substrates and maintaining the energy status of the cell.

3.6. ATM inhibition interfered with autophagy

Since autophagy acts as a cytoprotective effect in response to BO-1051-induced cell death, we explored whether the DNA-damage signaling pathway interacts with the autophagy pathway. Specifically, we wondered if the ATM signaling pathway interconnects with autophagy and if an ATM kinase inhibitor could contribute to autophagy. Thus, we examined the expression levels of p62/SQSTM1 and LC3 after ATM kinase inhibitor treatment (Fig. 5A). Surprisingly, we found that the ATM kinase inhibitor increased LC3-II and p62/SQSTM1 levels in the absence of BO-1051. To confirm whether the ATM kinase inhibitor increases autophagic flux, we applied protease inhibitors and examined the quantity of LC3-II. As shown in Fig. 5B, LC3-II conversion significantly increased in the presence of protease inhibitors, despite the increased level of p62/SQSTM1. Therefore, the ATM kinase inhibitor induced on-rate autophagic flux.

Since the ATM kinase inhibitor induced on-rate autophagic flux, we speculated that the rescue effect might be partially contributed by autophagy. Therefore, we evaluated the rescue effect of the ATM kinase inhibitor during autophagy inhibition by knocking down Beclin-1 and investigating whether the ATM kinase inhibitor was still capable of rescuing cells in an autophagy-incompetent state. As shown in Fig. 5C, the ATM kinase inhibitor was sufficient to reduce the annexin V-positive population in the autophagy-inhibited group to the level of the shLuc control. These results suggest that autophagy induced by the ATM kinase inhibitor do not contribute the rescue effect. While there is no functional autophagy system, the ATM kinase inhibitor alone was sufficient to block the DNA damage-induced apoptotic pathway. Compared to the reduced survival effect contributed by autophagy inhibition, DNA damage-caused apoptosis was the major determinant of cell fate.

Previous studies indicate the prosurvival role of p62/SQSTM1 in protecting cells against apoptosis and oxidative stress-induced cell death [16,17]. In order to elucidate the role of p62/SQSTM1 accumulation induced by the ATM kinase inhibitor, we used siRNA to knockdown p62/SQSTM1 expression (Figs. S5 and 5D). There was no difference between the siCtrl and siSQSTM1 group when we estimated the annexin V-positive population after BO-1051 treatment. Therefore, p62/SQSTM1 accumulation induced by the ATM inhibitor does not contribute to the rescue effect. Moreover, p62/SQSTM1 does not play a significant role against BO-1051-induced cell toxicity.

Nevertheless, the ATM kinase inhibitor-triggered autophagic flux conflicted with the fact that the activation of the ATM signaling pathway accompanied BO-1051-induced autophagy. In order to clarify the effects of ATM, we used siRNA to specifically knockdown the expression of ATM. As shown in Fig. 5E, ATM knockdown did not influence the expression level of the autophagic markers, LC3-II and p62/SQSTM1. When cells were treated with BO-1051 combined with ATM knockdown, the expression level of p-mTOR and p62/SQSTM1 only slightly decreased, and the increase in LC3-II was less as compared to the siCTRL group. These data indicate that ATM does interconnect with autophagy, even though the opposite data were obtained using a different model. These data may also indicate that the side effects exist when using an ATM kinase inhibitor.

3.7. Autophagy acts as cytoprotective effect in response to other DNA-damage agents in liver cancer cell lines

Cisplatin and doxorubicin are traditional chemotherapeutics. As they have little or no effective response in liver cancer therapy [18], it is possible that these agents also induce autophagy in liver cancer and restrict their effectiveness. Thus, we tested this idea in HA22T/VGH and Mahlavu cells. Both doxorubicin and cisplatin induced ATM phosphorylation in HA22T/VGH and Mahlavu cells (Fig. 6A). We showed that doxorubicin induced autophagy in both cell lines (Fig. 6B), while cisplatin induced autophagy in HA22T/VGH cells, but had no effect in Mahlavu cells (Fig. 6C). Because of the intense red fluorescence of doxorubicin, we used Western blotting instead of annexin V staining to evaluate the effect of autophagy inhibition on cell survival. As shown in Fig. 6D and E, HA22T/VGH cells overexpressed shLuc or shBECN1. Autophagy inhibition by knocking down beclin-1 enhanced apoptosis. As cleaved PARP and cleaved caspase-3 both increased (Fig. 6E). The autophagy inhibitors, BafA1 and chloroquine, made both cell lines more susceptible to doxorubicin (Fig. 6F and G). Likewise, cisplatin resulted in an increased in the annexin V-positive population in both cell lines (Fig. 6H and I), even though only a basal level of autophagy was present in Mahlavu cells. From the data above, we demonstrate the significance of autophagy in HCC cell lines in response to DNA-targeting agents.

4. Discussion

In the present study, we showed that BO-1051, a newly synthesized N-mustard linked with DNA-affinic molecule, induces prominent cytotoxicity in HCC cell lines. Even though BO-1051 had been shown to exhibit promising ability to induce DNA double strand breaks, the downstream signaling mechanism of cell death has not been fully studied. We focused our attention on BO-1051-induced cell responses. We have demonstrated that BO-1051 induced apoptosis in HA22T/VGH and Mahlavu cells through a DNA-damage signaling pathway. Upon inhibition of ATM or Chk2, the apoptotic population was significantly reduced. While BO-1051 resulted in apparent apoptosis at the time point of 48 h after treatment, autophagy was observed as soon as 8 h after BO-1051 was added to the culture medium. The maturation of LC3-II indicated that the induction of autophagy was time-dependent, as it increased gradually until cells showed obvious signs of apoptosis.

Nevertheless, the role of autophagy is still controversial: it has been reported to be either prodeath or prosurvival [19]. In HCC cell lines, autophagy can be induced by various compounds and can be involved in cell death or cytoprotection, as suggested previously [6,9,10]. We therefore chose an autophagy inhibitor, BafA1, to investigate the role of autophagy in BO-1051-induced cell death. Our data revealed that this inhibitor could not prevent, but rather

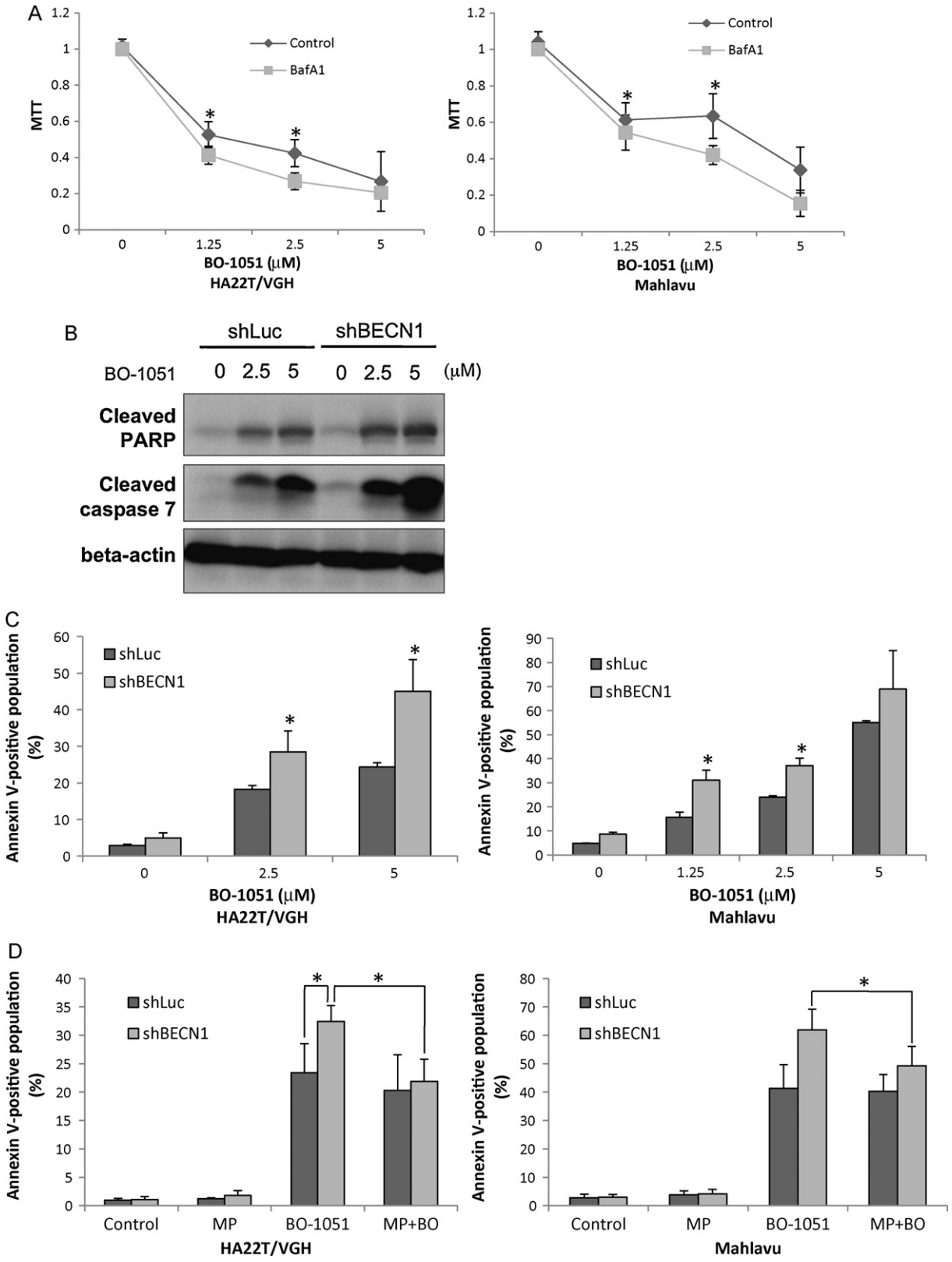

Fig. 4. Inhibition of autophagy could not prevent, but further enhanced, the cell death induced by BO-1051. (A) HA22T/VGH (left) and Mahlavu (right) cells were treated with BO-1051 at the indicated concentrations in the presence or absence of the autophagy inhibitor, BafA1 (10 nM), and cell viability was evaluated using the MTT assay. (B) HA22T/VGH cells overexpressing shLuc or shBECN1 were treated with different concentrations of BO-1051 for 48 h. Cells lysates were then subjected to immunoblotting with indicated antibodies. (C) HA22T/VGH (left) and Mahlavu (right) cells overexpressing shLuc or shBECN1 were treated with BO-1051 for 48 h and double-stained with annexin V-FITC and PI. (D) HA22T/VGH (left) and Mahlavu (right) cells were treated with either solvent or BO-1051 for 48 h. In the group with methyl pyruvate (MP) treatment, MP (10 mM) was added to the medium 24 h before analysis. Results shown are the mean ± SD of at least three independent experiments. $^*p < 0.05$.

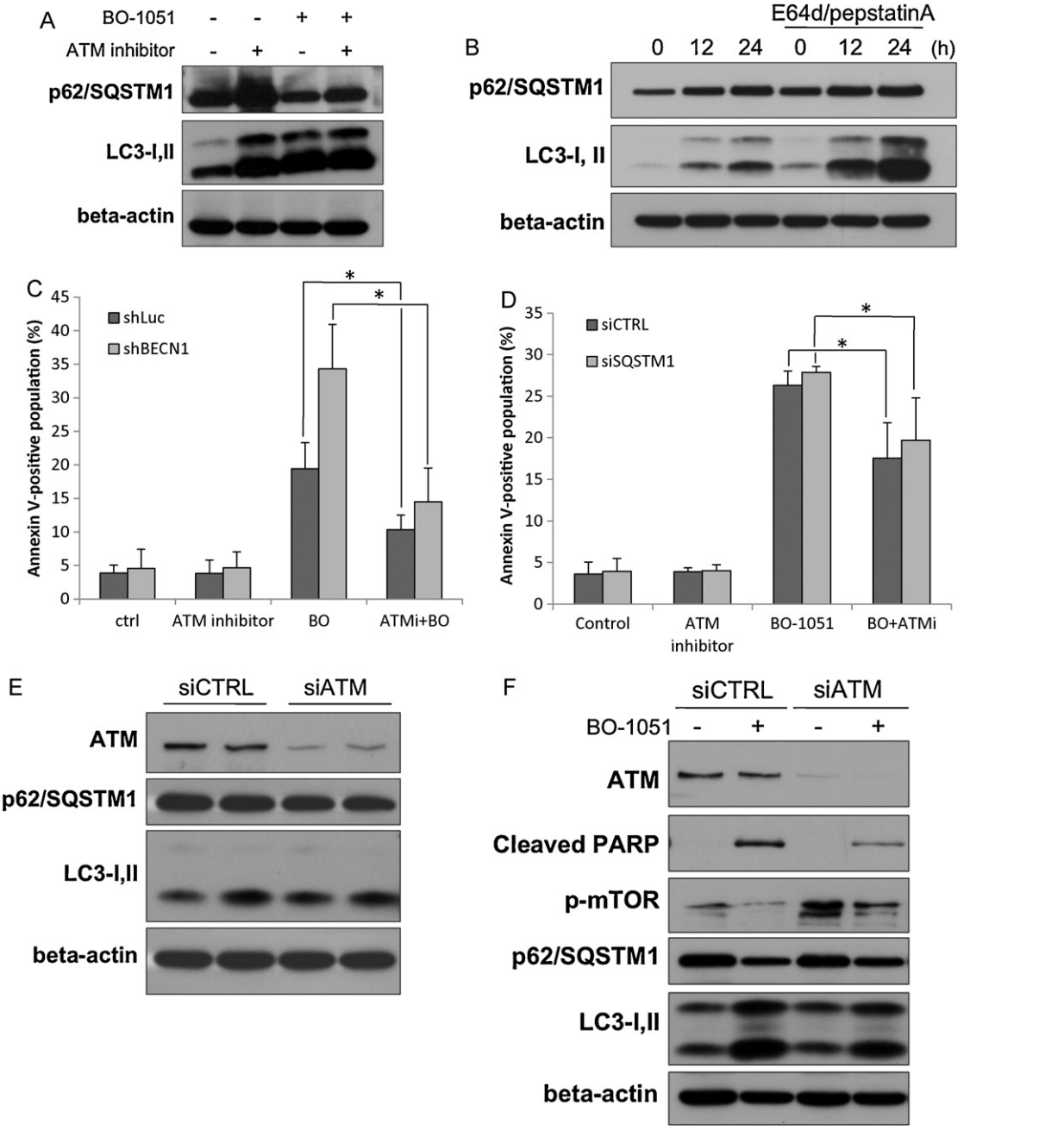

Fig. 5. ATM inhibition interfered with autophagy. (A) HA22T/VGH cells were treated with BO-1051 (5 μM), ATM kinase inhibitor (10 μM), or both, and cell lysates were subjected to immunoblotting with indicated antibodies. (B) HA22T/VGH cells were treated with an ATM kinase inhibitor (10 μM) for the indicated time, and extracted proteins were then immunoblotted with p62/SQSTM1 and LC3 antibodies. E64d (10 μg/ml) and pepstatin A (10 μg/ml) were added to the medium where indicated. (C) HA22T/VGH overexpressing with shLuc or shBECN1 were treated with BO-1051, ATM kinase inhibitor, or both, and subjected to annexin V-FITC staining. (D) After transfection of siCTRL or siSQSTM1, HA22T/VGH cells were treated with BO-1051 for 48 h and then subjected to annexin V-FITC and PI staining. (E) HA22T/VGH cells were transfected with siCTRL or siATM and stained with indicated antibodies. (F) After transfection of siCTRL or siATM, BO-1051 (5 μM) was added to the medium for 48 h to evaluate its effect. Results shown are the mean ± SD of three independent experiments. $^*p < 0.05$.

enhanced, BO-1051-induced cell death. Similarly, knockdown of Beclin-1 using a specific shRNA showed the same result. Although it has been reported that inhibition of autophagy at different stages has opposite effects on cell survival [11], we found that inhibition of autophagy leads to enhanced apoptosis in both early or late stages in our experiments. In consequence, autophagy may have a protective role in BO-1051-induced cell death, and is not strictly a prodeath mechanism. The reason that autophagy may be involved in cytoprotection can be explained with the experiments using methylpyruvate, which serves as an energy source. Cells with functional autophagy are able to degrade and recycle cellular constituents (long-lived proteins and organelles) and supply metabolic substrates for maintaining the energetic status. After DNA damage, autophagy may help to sustain the ATP concentration and therefore delay the onset of apoptotic cell death [12].

The role of ATM in cell death caused by DNA damage is well defined. Nevertheless, ATM was recently found to be involved in metabolic pathways other than DNA damage [20]. In addition, it has been reported that the knockout of ATM prevents the induction of autophagy in response to ROS in human lymphoblast cells [21]. Even though genotoxic stress is capable of inducing autophagy [8,12], direct evidence is still limited. Our results showed that the

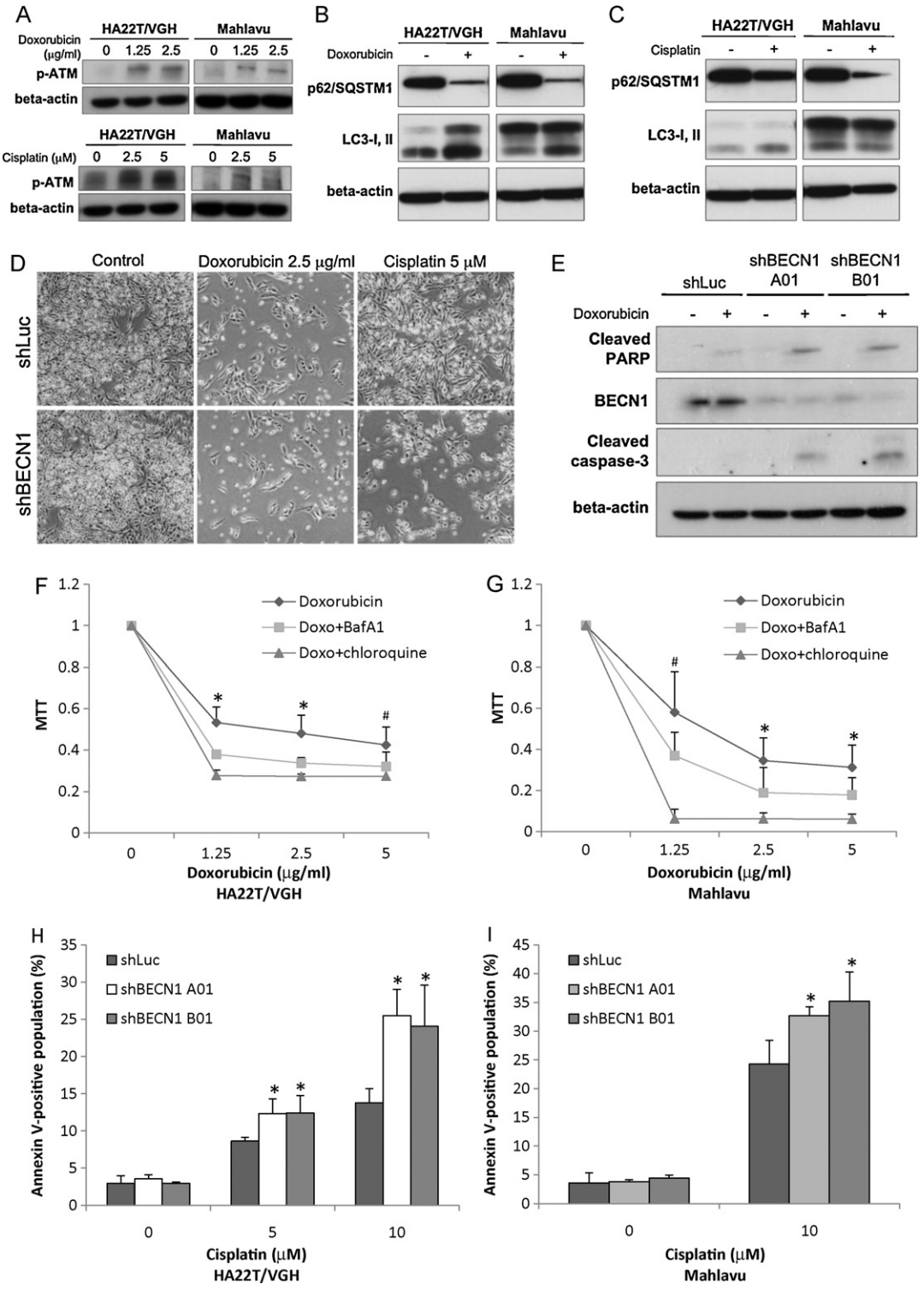

Fig. 6. Inhibition of autophagy sensitized cells to both cisplatin and doxorubicin. (A) HA22T/VGH and Mahlavu cells treated with solvent, doxorubicin, or cisplatin were immunoblotted with p-ATM-specific antibody to evaluate the activation of ATM. (B) HA22T/VGH and Mahlavu cells treated with solvent or doxorubicin (1.25 μg/ml) were immunoblotted with p62/SQSTM1- and LC3-specific antibodies to evaluate the induction of autophagy. (C) HA22T/VGH and Mahlavu cells were treated with solvent or cisplatin (5 μM), and cell lysates were then immunoblotted with antibodies against p62/SQSTM1 and LC3. (D) HA22T/VGH cells overexpressing shLuc or shBECN1 were treated with solvent, cisplatin or doxorubicin at the indicated concentration. After 48 h, cell morphology was observed. (E) HA22T/VGH cells overexpressing shLuc or shBECN1 were treated with doxorubicin. After 48 h, proteins were extracted and immunoblotted with anti-BECN1, anti-cleaved PARP, and anticleaved caspase-3 antibodies. (F) HA22T/VGH and (G) Mahlavu cells were treated with doxorubicin in the presence or absence of autophagy inhibitors, BafA1 or chloroquine. MTT assays were performed to evaluate cell viability. Data represent are three independent experiments and are shown as mean ± SD. $^{*}p < 0.05$ when compared to the other two groups. $^{\#}p < 0.05$ when compared to the group of doxorubicin plus chloroquine. (H) HA22T/VGH and (I) Mahlavu cells overexpressing shLuc or shBECN1 were treated with cisplatin for 48 h, followed by annexin V-FITC staining. Data represent three independent experiments and are shown as mean ± SD. $^{*}p < 0.05$. Bar = 100 μm.

ATM kinase inhibitor, combined with BO-1051 treatment, directly affects LC3-II conversion and p62/SQSTM1 degradation. Nevertheless, the effects of the ATM kinase inhibitor were opposite to the results obtained using siRNA to specifically knockdown ATM. While the ATM kinase inhibitor triggered autophagic flux, ATM knockdown had no effects on LC3-II or p62/SQSTM1 expression. The side effects of the ATM kinase inhibitor may contribute these conflicting results.

ATM knockdown made cells less responsive to BO-1051-triggered autophagy. This result suggests that ATM may serve as a direct link between DNA damage and autophagy. After DNA is damaged by various genotoxic stresses, the signal is passed to ATM, which then transduces the message to both apoptotic and autophagic pathways to activate cell death and cytoprotection mechanisms. On the other hand, autophagy may also regulate the DNA damage signaling pathway, as a study indicated that inhibition of mTOR (another regulator of autophagy) also leads to the upregulation of proteins involved in DNA damage responses [22]. Recently, Alexander et al. discovered that ATM can signal to TSC2 in the cytoplasm and subsequently regulate mTORC1 and autophagy activity [21]. These studies provide clues for possible connections between autophagy and the DNA-damage pathway. As illustrated in Fig. 6, DNA damage (induced by BO-1051 or other genotoxic stresses) could activate both apoptosis and autophagy in apoptosis-competent cells. In response to genotoxic stress, the induction of autophagy inhibits or delays the onset of apoptosis by providing metabolic substrates in HCC cell lines.

P62/SQSTM1 is selectively degraded via autophagy [23,24], is involved in the degradation of polyubiquitinated proteins, and plays a critical role in cell survival [25–27]. Recent studies emphasize that p62/SQSTM1 is an important mediator in promoting tumorigenesis [28] and serves as a marker for prostatic malignancy [29]. Several studies have indicated the prosurvival role of p62/SQSTM1 in protecting cells against apoptosis and oxidative stress-induced cell death [16,17]. Another study showed that p62/SQSTM1 is involved in the full activation of caspase-8 and the commitment to cell death [30]. In our study, in order to clarify the role of p62/SQSTM1 in cells treated with an ATM inhibitor, we used siRNA to knockdown the expression of p62/SQSTM1. The results showed that the existence of p62/SQSTM1 did not interfere with the effects caused by BO-1051. This result suggests that the degradation of p62/SQSTM1 in autophagy is not a critical event required for cell survival in BO-1051-induced cytotoxicity, and the result may be applied to other DNA-damaging agents.

In past decades, antitumor agents were evaluated in patients with unresectable HCC. The application of standard chemotherapy in HCC is restricted since no regimen has proven effective. HCC possesses high resistance against chemotherapy because of the high mutational load, multiple metabolic enzymes and multidrug resistance gene expression. Therefore, agents like cisplatin or doxorubicin have a responsive rate. Cisplatin induced autophagy in the U251 glioma cell line, esophageal squamous cell carcinoma cells, and renal tubular epithelial cells to protect against apoptosis [31–34], but the induction of autophagic cell death has also been reported [35]. Autophagic cardiomyocyte death is associated with doxorubicin-induced cardiotoxicity [36,37]. Nevertheless, the significance of cisplatin and doxorubicin has not been determined in HCC cell lines. We examined if autophagy also affects the effect of doxorubicin or cisplatin in HCC cell lines. As shown in Section 3, doxorubicin induced autophagy, while cisplatin upregulated LC-3II conversion in HA22T/VGH cells, but the basal level of conversion was maintained in Mahlavu cells. The inhibition of autophagy resulted in enhanced cell death in both groups. These data suggest that autophagy also serves as a critical defensive mechanism in HCC cell lines against common chemotherapeutic agents.

Acknowledgements

This study was supported by research grants from National Science Council-(NSC 97-3111-B-075-001-MY3, 97-2320-B-075-003-MY3), Taipei Veterans General Hospital (V97B1-006, E1-008, F-001), the Joint Projects of UTVGH (VGHUST 98-p1-01), Yen-Tjing-Ling Medical Foundation (96/97/98), National Yang-Ming University (Ministry of Education, Aim for the Top University Plan) & Genomic Center Project, Institute of Biological medicine (IBMS-CRC99-p01), Academia Sinica, and Center of Excellence for Cancer Research at Taipei Veterans General Hospital (DOH99-TD-C-111-007), Taiwan.

Appendix A. Supplementary data

Supplementary data associated with this article can be found, in the online version, at doi:10.1016/j.bcp.2010.12.011.

References

[1] Su TL, Lin YW, Chou TC, Zhang X, Bacherikov VA, Chen CH, et al. Potent antitumor 9-anilinoacridines and acridines bearing an alkylating N-mustard residue on the acridine chromophore: synthesis and biological activity. J Med Chem 2006;49:3710–8.
[2] Gourdie TA, Valu KK, Gravatt GL, Boritzki TJ, Baguley BC, Wakelin LP, et al. DNA-directed alkylating agents. 1. Structure-activity relationships for acridine-linked aniline mustards: consequences of varying the reactivity of the mustard. J Med Chem 1990;33:1177–86.
[3] Bacherikov VA, Chou TC, Dong HJ, Zhang X, Chen CH, Lin YW, et al. Potent antitumor 9-anilinoacridines bearing an alkylating N-mustard residue on the anilino ring: synthesis and biological activity. Bioorg Med Chem 2005;13:3993–4006.
[4] Kapuriya N, Kapuriya K, Zhang X, Chou TC, Kakadiya R, Wu YT, et al. Synthesis and biological activity of stable and potent antitumor agents, aniline nitrogen mustards linked to 9-anilinoacridines via a urea linkage. Bioorg Med Chem 2008;16:5413–23.
[5] Kanzawa T, Kondo Y, Ito H, Kondo S, Germano I. Induction of autophagic cell death in malignant glioma cells by arsenic trioxide. Cancer Res 2003;63:2103–8.
[6] Chang CP, Yang MC, Liu HS, Lin YS, Lei HY. Concanavalin A induces autophagy in hepatoma cells and has a therapeutic effect in a murine in situ hepatoma model. Hepatology 2007;45:286–96.
[7] Gorka M, Daniewski WM, Gajkowska B, Lusakowska E, Godlewski MM, Motyl T. Autophagy is the dominant type of programmed cell death in breast cancer MCF-7 cells exposed to AGS 115 and EFDAC, new sesquiterpene analogs of paclitaxel. Anticancer Drugs 2005;16:777–88.
[8] Abedin MJ, Wang D, McDonnell MA, Lehmann U, Kelekar A. Autophagy delays apoptotic death in breast cancer cells following DNA damage. Cell Death Differ 2007;14:500–10.
[9] Longo L, Platini F, Scardino A, Alabiso O, Vasapollo G, Tessitore L. Autophagy inhibition enhances anthocyanin-induced apoptosis in hepatocellular carcinoma. Mol Cancer Ther 2008;7:2476–85.
[10] Ko H, Kim YJ, Park JS, Park JH, Yang HO. Autophagy inhibition enhances apoptosis induced by ginsenoside Rk1 in hepatocellular carcinoma cells. Biosci Biotechnol Biochem 2009;73:2183–9.
[11] Kanzawa T, Germano IM, Komata T, Ito H, Kondo Y, Kondo S. Role of autophagy in temozolomide-induced cytotoxicity for malignant glioma cells. Cell Death Differ 2004;11:448–57.
[12] Katayama M, Kawaguchi T, Berger MS, Pieper RO. DNA damaging agent-induced autophagy produces a cytoprotective adenosine triphosphate surge in malignant glioma cells. Cell Death Differ 2007;14:548–58.
[13] Kitanaka C, Kuchino Y. Caspase-independent programmed cell death with necrotic morphology. Cell Death Differ 1999;6:508–15.
[14] Klionsky DJ, Abeliovich H, Agostinis P, Agrawal DK, Aliev G, Askew DS, et al. Guidelines for the use and interpretation of assays for monitoring autophagy in higher eukaryotes. Autophagy 2008;4:151–75.
[15] Lum JJ, Bauer DE, Kong M, Harris MH, Li C, Lindsten T, et al. Growth factor regulation of autophagy and cell survival in the absence of apoptosis. Cell 2005;120:237–48.
[16] Paine MG, Babu JR, Seibenhener ML, Wooten MW. Evidence for p62 aggregate formation: role in cell survival. FEBS Lett 2005;579:5029–34.
[17] Heo SR, Han AM, Kwon YK, Joung I. p62 protects SH-SY5Y neuroblastoma cells against H2O2-induced injury through the PDK1/Akt pathway. Neurosci Lett 2009;450:45–50.
[18] Carr BI. Hepatocellular carcinoma: current management and future trends. Gastroenterology 2004;127:S218–24.

[19] Ferraro E, Cecconi F. Autophagic and apoptotic response to stress signals in mammalian cells. Arch Biochem Biophys 2007;462:210–9.
[20] Schneider JG, Finck BN, Ren J, Standley KN, Takagi M, Maclean KH, et al. ATM-dependent suppression of stress signaling reduces vascular disease in metabolic syndrome. Cell Metab 2006;4:377–89.
[21] Alexander A, Cai SL, Kim J, Nanez A, Sahin M, MacLean KH, et al. ATM signals to TSC2 in the cytoplasm to regulate mTORC1 in response to ROS. Proc Natl Acad Sci USA 2010;107:4153–8.
[22] Bandhakavi S, Kim YM, Ro SH, Xie H, Onsongo G, Jun CB, et al. Quantitative nuclear proteomics identifies mTOR regulation of DNA damage response. Mol Cell Proteomics 2010;9:403–14.
[23] Pankiv S, Clausen TH, Lamark T, Brech A, Bruun JA, Outzen H, et al. p62/SQSTM1 binds directly to Atg8/LC3 to facilitate degradation of ubiquitinated protein aggregates by autophagy. J Biol Chem 2007;282:24131–45.
[24] Ichimura Y, Kominami E, Tanaka K, Komatsu M. Selective turnover of p62/A170/SQSTM1 by autophagy. Autophagy 2008;4:1063–6.
[25] Wooten MW, Geetha T, Babu JR, Seibenhener ML, Peng J, Cox N, et al. Essential role of sequestosome 1/p62 in regulating accumulation of Lys63-ubiquitinated proteins. J Biol Chem 2008;283:6783–9.
[26] Bjorkoy G, Lamark T, Brech A, Outzen H, Perander M, Overvatn A, et al. p62/SQSTM1 forms protein aggregates degraded by autophagy and has a protective effect on huntingtin-induced cell death. J Cell Biol 2005;171:603–14.
[27] Babu JR, Geetha T, Wooten MW. Sequestosome 1/p62 shuttles polyubiquitinated tau for proteasomal degradation. J Neurochem 2005;94:192–203.
[28] Mathew R, Karp CM, Beaudoin B, Vuong N, Chen G, Chen HY, et al. Autophagy suppresses tumorigenesis through elimination of p62. Cell 2009;137:1062–75.
[29] Kitamura H, Torigoe T, Asanuma H, Hisasue SI, Suzuki K, Tsukamoto T, et al. Cytosolic overexpression of p62 sequestosome 1 in neoplastic prostate tissue. Histopathology 2006;48:157–61.
[30] Jin Z, Li Y, Pitti R, Lawrence D, Pham VC, Lill JR, et al. Cullin3-based polyubiquitination and p62-dependent aggregation of caspase-8 mediate extrinsic apoptosis signaling. Cell 2009;137:721–35.
[31] Harhaji-Trajkovic L, Vilimanovich U, Kravic-Stevovic T, Bumbasirevic V, Trajkovic V. AMPK-mediated autophagy inhibits apoptosis in cisplatin-treated tumor cells. J Cell Mol Med 2009.
[32] Kaushal GP, Kaushal V, Herzog C, Yang C. Autophagy delays apoptosis in renal tubular epithelial cells in cisplatin cytotoxicity. Autophagy 2008;4:710–2.
[33] Periyasamy-Thandavan S, Jiang M, Wei Q, Smith R, Yin XM, Dong Z. Autophagy is cytoprotective during cisplatin injury of renal proximal tubular cells. Kidney Int 2008;74:631–40.
[34] Liu D, Yang Y, Liu Q, Wang J. Inhibition of autophagy by 3-MA potentiates cisplatin-induced apoptosis in esophageal squamous cell carcinoma cells. Med Oncol 2009.
[35] Spano A, Monaco G, Barni S, Sciola L. Cisplatin treatment of NIH/3T3 cultures induces a form of autophagic death in polyploid cells. Histol Histopathol 2008;23:717–30.
[36] Lu L, Wu W, Yan J, Li X, Yu H, Yu X. Adriamycin-induced autophagic cardiomyocyte death plays a pathogenic role in a rat model of heart failure. Int J Cardiol 2009;134:82–90.
[37] Zhang YW, Shi J, Li YJ, Wei L. Cardiomyocyte death in doxorubicin-induced cardiotoxicity. Arch Immunol Ther Exp (Warsz) 2009;57:435–45.